Photonic production of a pair of B_c mesons

A. E. Dorokhov
Joint Institute for Nuclear Research, BLTP, Moscow region, Dubna 141980, Russia

R. N. Faustov
Institute of Cybernetics and Informatics in Education, FRC CSC RAS, Moscow 119333, Russia

A. P. Martynenko and F. A. Martynenko
Samara National Research University, Samara 443086, Russia

(Received 20 May 2020; accepted 17 July 2020; published 31 July 2020)

We study the pair production of B_c mesons in the photon-photon interaction in the framework of perturbative quantum chromodynamics and the relativistic quark model. The production amplitudes of a pair of pseudoscalar and vector B_c mesons are constructed in the nonrelativistic approximation and taking into account relativistic effects. Relativistic corrections related to the relative motion of heavy quarks in the production amplitude, as well as in the wave function of the bound state of heavy quarks, are taken into account. Analytical expressions are constructed for the relativistic differential and total cross sections for the pair B_c meson production. Based on them, numerical values of the production cross sections are obtained for various energies and scattering angles.

DOI: 10.1103/PhysRevD.102.016027

I. INTRODUCTION

Among the various reactions that are studied at modern elementary particle accelerators, the processes of the creation of bound states of heavy quarks (b, c) hold a special place. This is due to the fact that various theoretical methods have been developed to study the properties of heavy quarkonia that have already proven their effectiveness. It cannot be said that the accuracy of theoretical calculations of the observed values for charmonium and others is very high. Nevertheless, different theoretical approaches allow us to calculate the mass spectrum, decay width, and production cross section of heavy quarkonia so that the obtained results generally describe experimental data [1–5]. Thus, interest in the processes of production of heavy quarks is connected primarily with the ability to test the quantum chromodynamics and the theory of bound states of particles. In this sense, interest to exclusive processes of pair production of heavy quarkonia is enhanced by the fact that the effects of quark coupling are manifested here to a greater extent [6–11]. Quarks are produced initially at short distances, almost free, and then diverge upon hadronization over long distances, at which the nonperturbative effects of their interaction become decisive. As already shown by the studies of the production of a pair of charmoniums, such reactions make it possible to identify shortcomings in theoretical calculations of the production cross sections and to search for new mechanisms of interaction between quarks and gluons.

The study of various physical reactions in $\gamma\gamma$-interaction has always been part of the physical research program at electron-positron colliders. Such reactions arise as a result of the interaction of a cloud of virtual photons that are associated with accelerated charged particles. The transition from virtual to real photons was made possible due to the Compton back scattering of laser light [12,13]. The production of high-energy real photons from light scattering by a 6-GeV electron beam, based on the Compton back scattering, was demonstrated in [14]. Scattered photons acquired energies of hundreds of MeV and propagated mainly in the same direction as the electrons of the initial beam. A new round of interest in $\gamma\gamma$ interaction is currently connected primarily with the discovery of the Higgs boson, with the study of the $\gamma\gamma \to H$ process and the construction of the Higgs factory. The luminosity of the photon collider turns out to be related to the luminosity of the e^+e^- collider by the relation: $L_{\gamma\gamma} = k^2 L_{ee}$, where the parameter k is defined as the fraction of electrons that produce the Compton photon. While e^+e^- colliders have proven themselves in the study of various particle interactions, the creation of a photon collider together with the linear e^+e^- collider, in which electron beams are converted to the photon beams, will allow us to conduct more effective research in a number of directions [15,16]. The study of different physical processes in which a pair of B_c mesons can be produced is important for understanding the possibilities of experimental detection of these particles.

The production of B_c mesons is of particular interest in such reactions, since quarks of various flavors and masses arise in a bound state. Despite intensive experimental studies of B_c mesons, information on them remains rather scarce. In fact, only the ground state of B_c mesons (0^-) and the first excited state were observed. Single and paired production of B_c mesons in e^+e^- annihilation, pp interaction have already been studied for a long time both within the framework of the quark model and in nonrelativistic quantum chromodynamics. The first works on the single production of B_c mesons in the $\gamma\gamma$ interaction were performed in [17,18] taking into account relativistic effects. The production of B_c meson pair in pp and $\gamma\gamma$ interaction was estimated in [19]. In our previous works [20,21], the pair production of B_c mesons in electron-positron annihilation was studied, and we considered both one-photon and two-photon pair production mechanisms. In this paper, we consider the production of a pair of B_c mesons in a collision of two real photons. The collision of high-energy photons, which can be obtained by the Compton back scattering of laser photons by high-energy electrons, can cause the exclusive production of a pair of heavy quarkonia. Since previous studies of the production of quarkonia have revealed the important role of relativistic effects, we study the process $\gamma + \gamma \to B_c^+ + B_c^-$ both in the nonrelativistic approximation and taking into account relativistic corrections within our approach based on perturbative quantum chromodynamics and relativistic quark model [9,20,21].

II. GENERAL FORMALISM

The B_c meson is the bound state of two heavy quark and anti-quark $(\bar{b}, c)$ or $(b, \bar{c})$. At present, the ground state $B_c(0^-)$ with the mass $M_{B_c} = 6274.9 \pm 0.8$ MeV [22] and two excited states $B_c(2^1S_0)^+$ with mass $6872.1 \pm 1.3(\mathrm{stat}) \pm 0.1(\mathrm{syst}) \pm 0.8(B_c^+)$ MeV and $B_c(2^3S_1)^+$ with mass $6841.2 \pm 0.6(\mathrm{stat}) \pm 0.1(\mathrm{syst}) \pm 0.8(B_c^+)$ MeV have been discovered [22–24]. A new precision measurement of the B_c^+ meson mass is performed using proton-proton collision data collected with the LHCb experiment in [25]. For pair production of B_c mesons, it is necessary to have a reaction in which two quark-antiquark pairs $(c\bar{c})$ and $(b\bar{b})$ would initially be produced. The reaction $\gamma + \gamma \to B_c^+ + B_c^-$ that we study is determined by the 20 Feynman amplitudes, some of which are shown in Fig. 1. The Appendix A presents the entire set of production amplitudes of free quarks (b, c) and antiquarks $(\bar{b}, \bar{c})$ in the leading order of α_s, necessary for the subsequent production of a pair of B_c mesons. These amplitudes are generated in the FeynArts package [26,27]. The transition from the

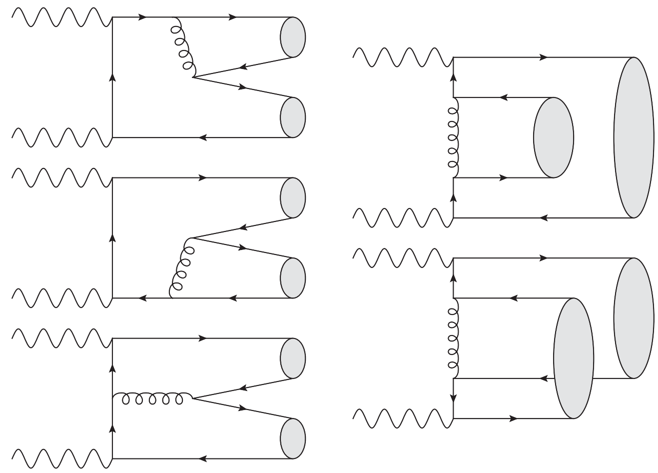

FIG. 1. The pair B_c-meson production amplitudes in $\gamma\gamma$ interaction. Wavy lines show the real photons with four momenta k_1 and k_2. Produced mesons B_c^+ and B_c^- in the final state are indicated by a hatched oval.

process of creating a pair of B_c mesons in e^+e^- annihilations to $\gamma\gamma$ interaction, therefore, leads to a significant increase in the number of amplitudes and complicates the calculation of the pair production cross section.

The general expression for the total production amplitude of a pair of B_c mesons can be written as a convolution of the production amplitude of two quarks (b, c), two antiquarks $(\bar{b}, \bar{c})$ in photon-photon collision, and quasipotential relativistic wave functions of B_c mesons [28,29]:

$$\mathcal{M}(k_1, k_2, P, Q) = \int \frac{d\mathbf{p}}{(2\pi)^3} \Psi_{\mathcal{V},\mathcal{P}}(p, P) \times \int \frac{d\mathbf{q}}{(2\pi)^3} \Psi_{\mathcal{V},\mathcal{P}}(q, Q) \mathcal{T}(p, q, P, Q), \quad (1)$$

where k_1, k_2 are four momenta of initial photons, P, Q are four momenta of final mesons. $\mathcal{T}(p, q, P, Q)$ is the production amplitude of four free quarks and antiquarks in $\gamma\gamma$ interaction, $\Psi_{\mathcal{V},\mathcal{P}}(p, P)$ is the wave function of B_c meson. A superscript $\mathcal{P}$ indicates a pseudoscalar B_c meson, a superscript $\mathcal{V}$ indicates a vector B_c meson. Four-momenta of the produced quarks and antiquarks can be expressed through total and relative four-momenta in the form:

$$p_1 = \eta_1 P + p, \quad p_2 = \eta_2 P - p, \quad (p \cdot P) = 0,$$
$$\eta_{1,2} = \frac{M_{B_c}^2 \pm m_1^2 \mp m_2^2}{2M_{B_c}^2},$$
$$q_1 = \rho_1 Q + q, \quad q_2 = \rho_2 Q - q, \quad (q \cdot Q) = 0,$$
$$\rho_{1,2} = \frac{M_{B_c}^2 \pm m_1^2 \mp m_2^2}{2M_{B_c}^2}, \quad (2)$$

where M_{B_c} is the mass of pseudoscalar or vector B_c^+ (B_c^{*+}) meson. Relative four-momenta of quarks $p = L_P(0, \mathbf{p})$ and $q = L_P(0, \mathbf{q})$ are obtained from the rest frame four-momenta $(0, \mathbf{p})$ and $(0, \mathbf{q})$ by the Lorentz transformation to the system moving with the momenta P and Q. Relativistic coefficients $\eta_{1,2}$ and $\rho_{1,2}$ are taken in such a way that the following conditions of orthogonality are satisfied: $(pP) = 0$, $(qQ) = 0$. In the nonrelativistic approximation, when we neglect the binding energies of quarks in the meson, the coefficients $\rho_{1,2} \approx \eta_{1,2} \approx r_{1,2} = m_{1,2}/(m_1 + m_2)$. In what follows, we denote the mass of the b-quark m_1 and the mass of c-quark m_2. In the case of B_c mesons the values $r_1 = 0.76$, $r_2 = 0.24$ are very close to $\eta_1 = 0.77$, $\rho_1 = 0.77$, $\eta_2 = 0.23$, $\rho_2 = 0.23$. Therefore, the use of coefficients $r_{1,2}$ is justified. It greatly simplifies the form of intermediate expressions for amplitudes. It is useful to recall that in the Bethe-Salpeter approach the initial production amplitude has a form of convolution of the truncated amplitude with two Bethe-Salpeter (BS) B_c meson wave functions. The presence of the $\delta(p \cdot P)$ function in this case allows us to make the integration over relative energy p^0. In the rest frame of a bound state the condition $p^0 = 0$ allows to eliminate the relative energy from the BS wave function.

The amplitudes shown in Fig. 1 differ by replacing the lines of b-quarks and c-quarks, as well as by rearrangement of the initial photons. We present analytical formulas for some amplitudes in the form (one representative from subclasses of amplitudes shown in Fig. 1):

$$\mathcal{T}_1(p,q,P,Q) = 16\pi^2\alpha_{s,c}\alpha Q_b^2 \varepsilon_1^\mu(k_1)\varepsilon_2^\nu(k_2) D_{\lambda\sigma}^{ab}(l_1)\bar{u}_1^i(p_1)\gamma^\lambda T_{ij}^a \frac{\hat{r}-\hat{q}_1-m_1}{(r-q_1)^2-m_1^2}\gamma^\mu \times \frac{\hat{k}_2-\hat{q}_1+m_1}{(k_2-q_1)^2-m_1^2}\gamma^\nu v_1^j(q_1)\bar{u}_2^m(q_2)\gamma^\sigma T_{mn}^b v_2^n(p_2), \tag{3}$$

$$\mathcal{T}_2(p,q,P,Q) = 16\pi^2\alpha_{s,c}\alpha Q_b^2 \varepsilon_1^\mu(k_1)\varepsilon_2^\nu(k_2) D_{\lambda\sigma}^{ab}(l_1)\bar{u}_1^i(p_1)\gamma^\mu T_{ij}^a \frac{\hat{p}_1-\hat{k}_1-m_1}{(p_1-k_1)^2-m_1^2}\gamma^\nu \times \frac{\hat{p}_1-\hat{r}+m_1}{(p_1-r)^2-m_1^2}\gamma^\lambda v_1^j(q_1)\bar{u}_2^m(q_2)\gamma^\sigma T_{mn}^b v_2^n(p_2), \tag{4}$$

$$\mathcal{T}_3(p,q,P,Q) = 16\pi^2\alpha_{s,c}\alpha Q_b^2 \varepsilon_1^\mu(k_1)\varepsilon_2^\nu(k_2) D_{\lambda\sigma}^{ab}(l_1)\bar{u}_1^i(p_1)\gamma^\mu T_{ij}^a \frac{\hat{p}_1-\hat{k}_1+m_1}{(p_1-k_1)^2-m_1^2}\gamma^\lambda \times \frac{\hat{k}_2-\hat{q}_1+m_1}{(k_2-q_1)^2-m_1^2}\gamma^\nu v_1^j(q_1)\bar{u}_2^m(q_2)\gamma^\sigma T_{mn}^b v_2^n(p_2), \tag{5}$$

$$\mathcal{T}_4(p,q,P,Q) = 16\pi^2\sqrt{\alpha_{s,c}\alpha_{s,b}}\alpha Q_c Q_b \varepsilon_1^\mu(k_1)\varepsilon_2^\nu(k_2) D_{\lambda\sigma}^{ab}(l_2)\bar{u}_1^i(p_1)\gamma^\mu T_{ij}^a \frac{\hat{p}_1-\hat{k}_1+m_1}{(p_1-k_1)^2-m_1^2}\gamma^\lambda v_1^j(q_1) \times \bar{u}_2^m(q_2)\gamma^\sigma T_{mn}^b \frac{\hat{k}_2-\hat{p}_2+m_2}{(k_2-p_2)^2-m_2^2}\gamma^\nu v_2^n(p_2), \tag{6}$$

$$\mathcal{T}_5(p,q,P,Q) = 16\pi^2\sqrt{\alpha_{s,c}\alpha_{s,b}}\alpha Q_c Q_b \varepsilon_1^\mu(k_1)\varepsilon_2^\nu(k_2) D_{\lambda\sigma}^{ab}(l_2)\bar{u}_1^i(p_1)\gamma^\mu T_{ij}^a \frac{\hat{p}_1-\hat{k}_1+m_1}{(p_1-k_1)^2-m_1^2}\gamma^\lambda v_1^j(q_1) \times \bar{u}_2^m(q_2)\gamma^\nu T_{mn}^b \frac{\hat{q}_2-\hat{k}_2+m_2}{(q_2-k_2)^2-m_2^2}\gamma^\sigma v_2^n(p_2), \tag{7}$$

where $l_1 = r - p_1 - p_1$, $l_2 = k_2 - p_2 - q_2$. $\varepsilon_1(k_1)$ and $\varepsilon_2(k_2)$ are the polarization vectors of initial photons. $D_{\lambda\sigma}^{ab}(l) = \delta^{ab} D_{\lambda\sigma}(l)$ is the gluon propagator. T^a is the SU(3) generator in the fundamental representation. The values of the strong coupling constant at different energies are indicated $\alpha_{s,c} = \alpha_s(\sqrt{s}\frac{m_2}{m_1+m_2})$ and $\alpha_{s,b} = \alpha_s(\sqrt{s}\frac{m_1}{m_1+m_2})$, $Q_c = 2/3$, and $Q_b = -1/3$ are the charges of heavy quarks, $u_{1,2}^i$, $v_{1,2}^j$ are wave functions of free quarks and antiquarks. Color factor is equal to $\frac{\delta_{ni}}{\sqrt{3}} T_{ij}^a T_{jk}^a \frac{\delta_{kn}}{\sqrt{3}} = \frac{4}{3}$ (the color part of the meson wave function is $\delta^{ik}/\sqrt{3}$).

Further transformation of the matrix elements in (1) is connected with the transformation law of the wave function of the bound state of quarks upon transition from the meson rest system to a moving reference frame with momenta Q and P. This law was obtained in the framework of the Bethe-Salpeter method in [30], and in the framework of the three-dimensional quasipotential approach in [31]. Since the quasipotential method is used in this work, the transformation of the wave function of mesons is represented as:

$$\Psi_P^{\rho\omega}(\mathbf{p}) = D_1^{1/2,\rho\alpha}(R_{L_P}^W)D_2^{1/2,\omega\beta}(R_{L_P}^W)\Psi_0^{\alpha\beta}(\mathbf{p}),$$
$$\bar{\Psi}_P^{\lambda\sigma}(\mathbf{p}) = \bar{\Psi}_0^{\varepsilon\tau}(\mathbf{p})D_1^{+1/2,\varepsilon\lambda}(R_{L_P}^W)D_2^{+1/2,\tau\sigma}(R_{L_P}^W), \quad (8)$$

where R^W is the Wigner rotation, L_P is the Lorentz boost from the meson rest frame to a moving one. The rotation matrix $D^{1/2}(R)$ is determined by

$$\begin{pmatrix} 1 & 0 \\ 0 & 1 \end{pmatrix} D_{1,2}^{1/2}(R_{L_P}^W) = S^{-1}(\mathbf{p}_{1,2})S(\mathbf{P})S(\mathbf{p}), \quad (9)$$

where the Lorentz transformation matrix of the Dirac spinor is

$$S(\mathbf{p}) = \sqrt{\frac{\epsilon(p)+m}{2m}}\left(1+\frac{(\boldsymbol{\alpha}\mathbf{p})}{\epsilon(p)+m}\right). \quad (10)$$

Further transformations of the amplitudes (3)–(7) entering in (1) should be carried out by means of the following expressions:

$$S_{\alpha\beta}(\Lambda)u_\beta^\lambda(p) = \sum_{\sigma=\pm 1/2} u_\alpha^\sigma(\Lambda p)D_{\sigma\lambda}^{1/2}(R_{\Lambda p}^W),$$
$$\bar{u}_\beta^\lambda(p)S_{\beta\alpha}^{-1}(\Lambda) = \sum_{\sigma=\pm 1/2} D_{\lambda\sigma}^{+1/2}(R_{\Lambda p}^W)\bar{u}_\alpha^\sigma(\Lambda p). \quad (11)$$

When constructing the production amplitudes of vector and pseudoscalar mesons, special projection operators on these states are used, which are constructed from the wave functions of quarks in the rest system. Therefore, the transformation formulas for Dirac bispinors of the following form are needed:

$$\bar{u}_1(\mathbf{p}) = \bar{u}_1(0)\frac{(\hat{p}_1'+m_1)}{\sqrt{2\epsilon_1(\mathbf{p})(\epsilon_1(\mathbf{p})+m_1)}}, \quad p_1' = (\epsilon_1, \mathbf{p}),$$
$$v_2(-\mathbf{p}) = \frac{(\hat{p}_2'-m_2)}{\sqrt{2\epsilon_2(\mathbf{p})(\epsilon_2(\mathbf{p})+m_2)}}v_2(0), \quad p_2' = (\epsilon_2, -\mathbf{p}). \quad (12)$$

After that we introduce the projection operators $\hat{\Pi}^{\mathcal{P},\mathcal{V}}$ on the heavy quark bound states $(c\bar{b})$, $(b\bar{c})$ with total spin 0 or 1:

$$\hat{\Pi}^{\mathcal{P},\mathcal{V}} = [v_2(0)\bar{u}_1(0)]_{s=0,1} = \gamma_5(\hat{\epsilon}^*)\frac{1+\gamma^0}{2\sqrt{2}}. \quad (13)$$

Total amplitude of pair B_c meson production can be presented after such transformations as follows:

$$\mathcal{M}(k_1,k_2,P,Q) = \frac{16\pi^2\alpha M_{\mathcal{V},\mathcal{P}}}{3}\int\frac{d\mathbf{p}}{(2\pi)^3}\int\frac{d\mathbf{q}}{(2\pi)^3} \times Sp\{\Psi_{B_c}^{\mathcal{V},\mathcal{P}}(p,P)\Gamma^{(1)}\Psi_{B_c}^{\mathcal{V},\mathcal{P}}(q,Q)\Gamma^{(2)}\}, \quad (14)$$

where $\Gamma^{(1,2)}$ are the vertex functions. For the amplitudes (3)–(7) they have the form:

$$\Gamma_{ij}^{(1)}\Gamma_{kl}^{(2)} = \Big\{\alpha_{s,c}Q_b^2D^{\lambda\sigma}(l_1)\left[\gamma^\lambda\frac{\hat{r}-\hat{q}_1+m_1}{(r-q_1)^2-m_1^2}\gamma^\mu\frac{\hat{k}_2-\hat{q}_1+m_1}{(k_2-q_1)^2-m_1^2}\gamma^\nu\right]_{ij}\gamma_{kl}^\sigma$$
$$+\alpha_{s,c}Q_b^2D^{\lambda\sigma}(l_1)\left[\gamma^\mu\frac{\hat{p}_1-\hat{k}_1+m_1}{(p_1-k_1)^2-m_1^2}\gamma^\nu\frac{\hat{p}_1-\hat{r}+m_1}{(p_1-r)^2-m_1^2}\gamma^\lambda\right]_{ij}\gamma_{kl}^\sigma$$
$$+\alpha_{s,c}Q_b^2D^{\lambda\sigma}(l_1)\left[\gamma^\mu\frac{\hat{p}_1-\hat{k}_1+m_1}{(p_1-k_1)^2-m_1^2}\gamma^\lambda\frac{\hat{k}_2-\hat{q}_1+m_1}{(k_2-q_1)^2-m_1^2}\gamma^\nu\right]_{ij}\gamma_{kl}^\sigma$$
$$+\sqrt{\alpha_{s,c}\alpha_{s,b}}Q_bQ_cD^{\lambda\sigma}(l_2)\left[\gamma^\mu\frac{\hat{p}_1-\hat{k}_1+m_1}{(p_1-k_1)^2-m_1^2}\gamma^\lambda\right]_{ij}\left[\gamma^\sigma\frac{\hat{k}_2-\hat{p}_2+m_2}{(k_2-p_2)^2-m_2^2}\gamma^\nu\right]_{kl}$$
$$+\sqrt{\alpha_{s,c}\alpha_{s,b}}Q_bQ_cD^{\lambda\sigma}(l_2)\left[\gamma^\mu\frac{\hat{p}_1-\hat{k}_1+m_1}{(p_1-k_1)^2-m_1^2}\gamma^\lambda\right]_{ij}\left[\gamma^\nu\frac{\hat{q}_2-\hat{k}_2+m_2}{(q_2-k_2)^2-m_2^2}\gamma^\sigma\right]_{kl}\Big\}\varepsilon_1^\mu(k_1)\varepsilon_2^\nu(k_2). \quad (15)$$

The transition wave functions $\Psi_{B_c^*}^{\mathcal{V}}(q,Q)$ and $\Psi_{B_c}^{\mathcal{P}}(p,P)$ (form factors) have the following form:

$$\Psi_{B_c}^{\mathcal{P}}(p,P) = \frac{\Psi_{B_c}^0(\mathbf{p})}{\sqrt{\frac{\epsilon_1(p)}{m_1}\frac{(\epsilon_1(p)+m_1)}{2m_1}\frac{\epsilon_2(p)}{m_2}\frac{(\epsilon_2(p)+m_2)}{2m_2}}}\left[\frac{\hat{v}_1-1}{2}+\hat{v}_1\frac{\mathbf{p}^2}{2m_2(\epsilon_2(p)+m_2)}-\frac{\hat{p}}{2m_2}\right]$$
$$\times\gamma_5(1+\hat{v}_1)\left[\frac{\hat{v}_1+1}{2}+\hat{v}_1\frac{\mathbf{p}^2}{2m_1(\epsilon_1(p)+m_1)}+\frac{\hat{p}}{2m_1}\right], \quad (16)$$

$$\Psi^{\mathcal{V}}_{B_c^*}(q,Q)=\frac{\Psi^0_{B_c^*}(\mathbf{q})}{\sqrt{\frac{\epsilon_1(q)}{m_1}\frac{(\epsilon_1(q)+m_1)}{2m_1}\frac{\epsilon_2(q)}{m_2}\frac{(\epsilon_2(q)+m_2)}{2m_2}}}\left[\frac{\hat{v}_2-1}{2}+\hat{v}_2\frac{\mathbf{q}^2}{2m_1(\epsilon_1(q)+m_1)}+\frac{\hat{q}}{2m_1}\right]$$
$$\times\hat{\varepsilon}_{\mathcal{V}}(Q,s_z)(1+\hat{v}_2)\left[\frac{\hat{v}_2+1}{2}+\hat{v}_2\frac{\mathbf{q}^2}{2m_2(\epsilon_2(q)+m_2)}-\frac{\hat{q}}{2m_2}\right], \tag{17}$$

where the four-vector p_μ convolution with the Dirac γ^μ matrix is indicated by $\hat{p}$, $v_1=P/M_{B_c}$, $v_2=Q/M_{B_c}$; $\varepsilon_{\mathcal{V}}(Q,s_z)$ is the polarization vector of the $B_c^{*-}(1^-)$ meson, relativistic quark energies $\epsilon_{1,2}(p)=\sqrt{p^2+m_{1,2}^2}$. The matrix element (14) contains the integration over the quark relative momenta $\mathbf{p}$ and $\mathbf{q}$. The result of the integration in (14) is determined by the bound state wave function but not the substitutions $M_{B_c}=\epsilon_1(\mathbf{p})+\epsilon_2(\mathbf{p})$ and $M_{B_c^*}=\epsilon_1(\mathbf{q})+\epsilon_2(\mathbf{q})$. Expressions (16) and (17) include the meson wave functions in the rest frame $\Psi^0_{B_c}(\mathbf{p})$ and spin projection operators with relativistic factors of quarks. Another form of spin projector for $(c\bar{c})$ system was used in [32] with heavy quark momenta lying on the mass shell. The functions (16)–(17) describe a transition of heavy quark-antiquark pair from free state to the bound state, so, they can be called the transition form factors. It is important to emphasize that a relativistic consideration of the production and decay of heavy quarkonia is necessary to obtain the values of the observed quantities [8,9,33,34].

We have also the dependence on relative momenta p and q in vertex functions $\Gamma^{(1)}$, $\Gamma^{(2)}$. The denominators of expression (15) can be simplified as follows:

$$(r-q_1)^2-m_1^2\approx r^2-2r_1rQ-2rq\approx r_2s,\,(k_1-q_1)^2-m_1^2\approx -r_1\sqrt{s}(P^0+|\mathbf{P}|\cos\theta),$$
$$(k_2-q_1)^2-m_1^2\approx -2r_1k_2Q=-2r_1k_1P=-r_1\sqrt{s}(P^0-|\mathbf{P}|\cos\theta), \tag{18}$$

where θ is the angle between photon $\mathbf{k}_1$ and meson $\mathbf{P}$ three momenta. so, we neglect here relative momenta p and q because corresponding corrections have the form p^2/s, q^2/s and are very small in size at $\sqrt{s}>2M_{B_c}$. We take into account exactly the corrections $p^2/m_{1,2}^2$, $q^2/m_{1,2}^2$ in the numerator of relativistic amplitudes.

The appearance of a large number of the Feynman amplitudes describing the production of a pair of B_c mesons makes the use of the FORM package [35] especially important. The total contribution of 20 amplitudes is conveniently represented as a sum of 5 parts, since 4 of 20 amplitudes each have a similar mathematical structure. The total amplitudes of pair production can be represented as a result in the form:

$$\mathcal{T}_{\mathcal{PP}}=\mathcal{T}^{\mu\nu}_{\mathcal{PP}}\varepsilon_1^\mu(k_1)\varepsilon_2^\nu(k_2),$$
$$\mathcal{T}^{\mu\nu}_{\mathcal{PP}}=\frac{A_1^{\mu\nu}}{r_1^3r_2^3s^{5/2}(P^0-|\mathbf{P}|z)}+\frac{A_2^{\mu\nu}}{r_1^2r_2^2s^2(P^0-|\mathbf{P}|z)^2}+\frac{A_3^{\mu\nu}}{r_1^3r_2^3s^{5/2}(P^0+|\mathbf{P}|z)}+\frac{A_4^{\mu\nu}}{r_1^2r_2^2s^2(P^0+|\mathbf{P}|z)^2}+\frac{A_5^{\mu\nu}}{r_1^2r_2^2s^2(P^0-|\mathbf{P}|z)(P^0+|\mathbf{P}|z)}, \tag{19}$$

$$\mathcal{T}_{\mathcal{VV}}=\mathcal{T}^{\mu\nu\epsilon_1\epsilon_2}_{\mathcal{VV}}\varepsilon_1^\mu(k_1)\varepsilon_2^\nu(k_2)\varepsilon_{\mathcal{V}}^{\epsilon_1}(P)\varepsilon_{\mathcal{V}}^{\epsilon_2}(Q),$$
$$\mathcal{T}^{\mu\nu\epsilon_1\epsilon_2}_{\mathcal{VV}}=\frac{B_1^{\mu\nu\epsilon_1\epsilon_2}}{r_1^3r_2^3s^{5/2}(P^0-|\mathbf{P}|z)}+\frac{B_2^{\mu\nu\epsilon_1\epsilon_2}}{r_1^2r_2^2s^2(P^0-|\mathbf{P}|z)^2}+\frac{B_3^{\mu\nu\epsilon_1\epsilon_2}}{r_1^3r_2^3s^{5/2}(P^0+|\mathbf{P}|z)}+\frac{B_4^{\mu\nu\epsilon_1\epsilon_2}}{r_1^2r_2^2s^2(P^0+|\mathbf{P}|z)^2}+\frac{B_5^{\mu\nu\epsilon_1\epsilon_2}}{r_1^2r_2^2s^2(P^0-|\mathbf{P}|z)(P^0+|\mathbf{P}|z)}, \tag{20}$$

where $\varepsilon_1^\mu(k_1)$, $\varepsilon_2^\nu(k_2)$, $\varepsilon_{\mathcal{V}}^{\epsilon_1}(P)$ are the polarization vectors of photons and vector meson, $z=\cos\theta$. We introduce the angle θ between the photon momentum $\mathbf{k_1}$ and momentum $\mathbf{P}$ of B_c meson. The tensors appearing in (19), (20) are very cumbersome when taking into account relativistic corrections. In the Appendix B, we write out the explicit form of these functions in the case of the production of a pair of pseudoscalar mesons.

To calculate the cross section we have to sum the squared modulus of the amplitude upon all polarizations using the following relations for final vector mesons and initial photons correspondingly ($v_1=P/M_{B_c}$, $v_2=Q/M_{B_c}$):

$$\sum_\lambda\varepsilon_P^{(\lambda)\mu}\varepsilon_P^{*(\lambda)\nu}=v_1^\mu v_1^\nu-g^{\mu\nu},\quad \sum_\lambda\varepsilon_Q^{(\lambda)\mu}\varepsilon_Q^{*(\lambda)\nu}=v_2^\mu v_2^\nu-g^{\mu\nu},\quad \sum_\lambda\varepsilon_{1,2}^{(\lambda)\mu}\varepsilon_{1,2}^{*(\lambda)\nu}=\frac{k_1^\mu k_2^\nu+k_1^\nu k_2^\mu}{k_1\cdot k_2}-g^{\mu\nu}. \tag{21}$$

After calculating the squared amplitude modulus, we obtain the differential effective cross section $d\sigma/d\cos\theta$ ($z = \cos\theta$)

$$d\sigma = \frac{1}{16\pi}|\mathcal{M}|^2 \frac{|\mathbf{P}|}{s^{3/2}} dz \tag{22}$$

as a function of center-of-mass energy $\sqrt{s}$. It depends on a number of parameters including heavy quark masses and relativistic corrections. $|\mathbf{P}| = \sqrt{(s-4M_{B_c}^2)/4}$ is the meson three momentum in center-of-mass frame. The technique of further transformations of $|\mathcal{M}|^2$ is described in detail in our previous works [20,21]. Let us briefly repeat the basic elements of our transformations and the used quark model. One of the very important parameters on which the numerical value of the production cross section depends (the cross section is proportional to the 4th power of this parameter) is the value of the bound state wave function at the origin. In the framework of the relativistic quark model, we have the following generalization of the nonrelativistic value $\Psi^{0,nr}_{B_c}(0)$:

$$\Psi^0_{B_c}(0) = \int \sqrt{\frac{(\epsilon_1(p)+m_1)(\epsilon_2(p)+m_2)}{2\epsilon_1(p)\cdot 2\epsilon_2(p)}} \Psi^0_{B_c}(\mathbf{p}) \frac{d\mathbf{p}}{(2\pi)^3}. \tag{23}$$

After the trace calculation in (14) we preserve in $|\mathcal{M}|^2$ only relativistic corrections proportional to second degree of $\mathbf{p}$ and $\mathbf{q}$. Next we express $\mathbf{p}^2$, $\mathbf{q}^2$ in powers of relativistic factors $C_{nk} = [(m_1-\epsilon_1(p))/(m_1+\epsilon_1(p))]^n[(m_2-\epsilon_2(q))/(m_2+\epsilon_2(q))]^k$ (n, k are integers and half-integers with $n+k \leq 1$):

$$\frac{\mathbf{p}^2}{4m_1^2} = \left(\frac{\epsilon_1-m_1}{\epsilon_1+m_1}\right)^{1/2} + \left(\frac{\epsilon_1-m_1}{\epsilon_1+m_1}\right)^{3/2} + \left(\frac{\epsilon_1-m_1}{\epsilon_1+m_1}\right)^{5/2}\ldots, \tag{24}$$

$$\frac{\mathbf{p}^2}{4m_2^2} = \left(\frac{\epsilon_2-m_2}{\epsilon_2+m_2}\right)^{1/2} + \left(\frac{\epsilon_2-m_2}{\epsilon_2+m_2}\right)^{3/2} + \left(\frac{\epsilon_2-m_2}{\epsilon_2+m_2}\right)^{5/2}\ldots, \tag{25}$$

$$\frac{\mathbf{p}^2}{4m_1m_2} = \left(\frac{(\epsilon_1-m_1)(\epsilon_2-m_2)}{(\epsilon_1+m_1)(\epsilon_2+m_2)}\right)^{1/2}\left[1 + \frac{(\epsilon_1-m_1)}{(\epsilon_1+m_1)} + \frac{(\epsilon_2-m_2)}{(\epsilon_2+m_2)} + \cdots\right]. \tag{26}$$

Last equation (26) is used to maintain the symmetry over quarks 1 and 2 in some terms. Finally, we introduce special relativistic parameters ω_{nk} which are defined as follows in terms of momentum integrals I^{nk} and calculated in the quark model:

$$I^{nk}_{B_c} = \int_0^\infty q^2 R_{B_c}(q) \sqrt{\frac{(\epsilon_1(q)+m_1)(\epsilon_2(q)+m_2)}{2\epsilon_1(q)\cdot 2\epsilon_2(q)}} \left(\frac{\epsilon_1(q)-m_1}{\epsilon_1(q)+m_1}\right)^n \left(\frac{\epsilon_2(q)-m_2}{\epsilon_2(q)+m_2}\right)^k dq, \tag{27}$$

$$\omega^{B_c}_{10} = \frac{I^{10}_{B_c}}{I^{00}_{B_c}}, \qquad \omega^{B_c}_{01} = \frac{I^{01}_{B_c}}{I_{B_c}}, \qquad \omega^{B_c}_{\frac{1}{2}\frac{1}{2}} = \frac{I^{\frac{1}{2}\frac{1}{2}}_{B_c}}{I^{00}_{B_c}}, \tag{28}$$

where $R_{B_c}(q)$ is the radial wave function of the B_c mesons in momentum space. With a good degree of accuracy, the main contribution to expansions (24)–(26) is made by the first terms, which we retain when calculating the cross sections.

Up to this point we have discussed the first group of relativistic corrections to the pair B_c meson production amplitude (14). As already noted they are connected with terms in (14) containing momenta of relative motion $\mathbf{p}$ and $\mathbf{q}$. But there exists another group of relativistic corrections which appear in the interaction operator of heavy quarks b and c and, as a result, in the bound state wave function $\Psi^0_{B_c}(\mathbf{p})$ in (16)–(17) [3,4,36–40]. For their calculation we use nonrelativistic Schrödinger equation in which the particle interaction operator

$$H = H_0 + \Delta U_1 + \Delta U_2, \quad H_0 = \sqrt{\mathbf{p}^2+m_1^2} + \sqrt{\mathbf{p}^2+m_2^2} - \frac{4\tilde{\alpha}_s}{3r} + (Ar+B), \tag{29}$$

consists of perturbative part $\Delta U_1(r)$ and $\Delta U_2(r)$:

$$\Delta U_1(r) = -\frac{\alpha_s^2}{3\pi r}[2\beta_0 \ln(\mu r) + a_1 + 2\gamma_E\beta_0], \quad a_1 = \frac{31}{3} - \frac{10}{9}n_f, \quad \beta_0 = 11 - \frac{2}{3}n_f, \tag{30}$$

TABLE I. Relativistic parameters entering in the production cross sections.

B_c meson	$n^{2S+1}L_J$	M_{B_c}, GeV	$\Psi^0_{B_c}(0)$, GeV$^{3/2}$	ω_{10}	ω_{01}	$\omega_{\frac{11}{22}}$
B_c	1^1S_0	6.276	0.250	0.0489	0.0060	0.0171
B_c^*	1^3S_1	6.317	0.211	0.0540	0.0066	0.0188

$$\Delta U_2(r) = -\frac{2\alpha_s}{3m_1m_2r}\left[\mathbf{p}^2+\frac{\mathbf{r}(\mathbf{rp})\mathbf{p}}{r^2}\right]+\frac{2\pi\alpha_s}{3}\left(\frac{1}{m_1^2}+\frac{1}{m_2^2}\right)\delta(\mathbf{r})+\frac{4\alpha_s}{3r^3}\left(\frac{1}{2m_1^2}+\frac{1}{m_1m_2}\right)(\mathbf{s}_1\mathbf{L})$$
$$+\frac{4\alpha_s}{3r^3}\left(\frac{1}{2m_2^2}+\frac{1}{m_1m_2}\right)(\mathbf{s}_2\mathbf{L})+\frac{32\pi\alpha_s}{9m_1m_2}(\mathbf{s}_1\mathbf{s}_2)\delta(\mathbf{r})+\frac{4\alpha_s}{m_1m_2r^3}\left[\frac{(\mathbf{s}_1\mathbf{r})(\mathbf{s}_2\mathbf{r})}{r^2}-\frac{1}{3}(\mathbf{s}_1\mathbf{s}_2)\right]$$
$$-\frac{\alpha_s^2(m_1+m_2)}{m_1m_2r^2}\left[1-\frac{4m_1m_2}{9(m_1+m_2)^2}\right], \tag{31}$$

and nonperturbative interaction $Ar+B+\Delta V^{hfs}_{\rm conf}(r)$:

$$\Delta V^{hfs}_{\rm conf}(r) = f_V\frac{A}{8r}\left\{\frac{1}{m_1^2}+\frac{1}{m_2^2}+\frac{16}{3m_1m_2}(\mathbf{s}_1\mathbf{s}_2)+\frac{4}{3m_1m_2}[3(\mathbf{s}_1\mathbf{r})(\mathbf{s}_2\mathbf{r})-(\mathbf{s}_1\mathbf{s}_2)]\right\}, \tag{32}$$

where an additional parameter is taken equal to $f_V = 0.9$, $\mathbf{L} = [\mathbf{r}\times\mathbf{p}]$, $\mathbf{s}_1$, $\mathbf{s}_2$ are spins of heavy quarks, n_f is the number of flavors, the Euler constant $\gamma_E \approx 0.577216$. All parameters of the quark interaction operator (29)–(32) were fixed as in previous papers [20,21].

Solving the Schrödinger equation numerically with the account terms (30)–(32), we obtain the wave function of the bound state $(b\bar{c})$ with spin $S=0$ and 1. Using this solution, numerical values of parameters (23) and (28) are calculated and presented in the Table I. The plots in Fig. 2 show the type of differential effective production cross sections for a pair of B_c mesons without and taking into account relativistic corrections. A significant decrease in the production cross sections taking into account relativistic corrections with respect to nonrelativistic cross sections is explained primarily by the decrease in the relativistic case in our model of the key parameter $\Psi^0_{B_c}(0)$. The ratio $|\Psi^{0,nr}_{B_c}(0)|^4/||\Psi^0_{B_c}(0)|^4$ for the states with spin 0 and 1, which is 2.4 and 4.8, respectively, shows how many times the nonrelativistic cross section decreases due to this factor.

Table I shows the masses of B_c mesons (the states $^1S_0$, $^3S_1$) obtained in our model. They are in good agreement with both the experimental result $M(1^1S_0) = 6.2749$ GeV [22] and theoretical calculations $M(1^3S_1) = 6.332$ GeV [3]. It should be emphasized the multidirectional effect of various relativistic corrections. Those relativistic corrections $\mathbf{p}^2/m^2_{1,2}$, $\mathbf{q}^2/m^2_{1,2}$ that are taken into account in the production amplitudes (19)–(20) give an increase in the production cross sections from 20 to 50% for different mesons. But relativistic corrections in the interaction potential of heavy quarks lead to a significant decrease

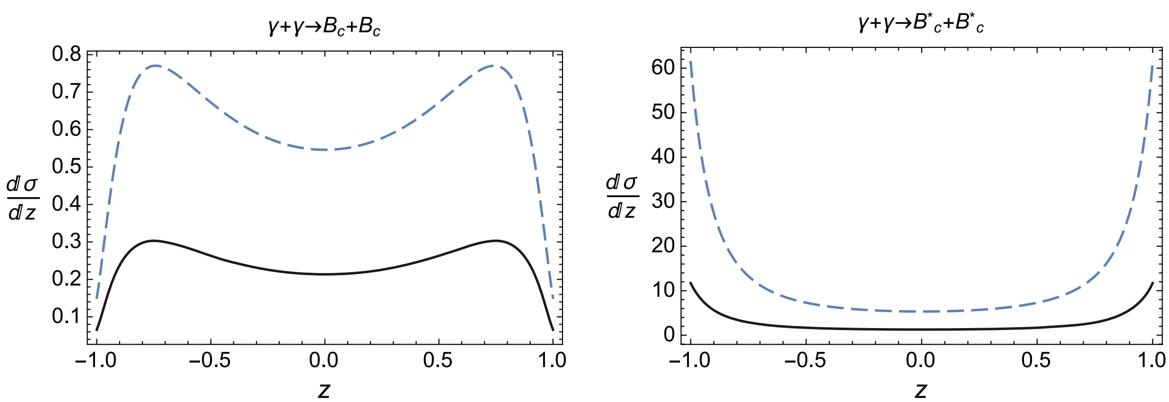

FIG. 2. The differential cross sections $d\sigma/dz$ ($z=\cos\theta$) in fb of pair B_c meson production in $\gamma\gamma$ interaction at the center-of-mass energy $\sqrt{s} = 20$ GeV (solid line). The dashed line shows nonrelativistic result.

in $\Psi^0_{B_c}(0)$ and, accordingly, to a decrease in the production cross sections. In general, this last factor is decisive.

III. NUMERICAL RESULTS AND CONCLUSION

While charmonium states have already been studied in sufficient detail, new excited states are being discovered, experimental data on the bound states $(c\bar{b})$, $(\bar{c}b)$ are rather small. Therefore, the search for various physical processes for their observation is an important task. The creation of a photonic collider based on ILC is of undoubted interest. The use of beams of real high-energy photons will allow us to study new processes of particle interaction and to verify existing theoretical models to describe them. One of these discussed processes is connected with the production of the Higgs boson and the study of various channels for its decay. Another promising direction of the $\gamma\gamma$ interaction, which is studied in this work, is related to the production of bound states of heavy quarks. The process of exclusive production of a pair of doubly heavy mesons or baryons is an important source of information on the interaction of heavy quarks. It can be used both to verify existing models for describing the bound states of particles, and to refine the values of the fundamental parameters of the theory. All particles generated in this reaction can be reliably identified by their decay products. Our relativistic approach to the study of quarkonium pair production reactions, formulated in [9,10,20,21], is extended in this work to a new process $\gamma+\gamma\to B_c^+ + B_c^-$.

We obtain leading order relativistic amplitudes (1), (19), (20) for the exclusive pair production of pseudoscalar and vector B_c mesons using the perturbative QCD and relativistic quark model. Taking into account the smallness of relative momenta of heavy quarks we make an expansion of the amplitude on p and q and hold the terms of the second order. There are two types of relativistic corrections related to the expansion in small parameters $\mathbf{p}^2/m^2_{1,2}$, $\mathbf{q}^2/m^2_{1,2}$ and $\mathbf{p}^2/s$, $\mathbf{q}^2/s$. The second type of corrections occurs when the denominators of the heavy quark propagators are expanded at small relative momenta p, q. We neglect the corrections of the form $\mathbf{p}^2/s$, $\mathbf{q}^2/s$ since at energies $\sqrt{s}>15$ GeV their numerical value is an order of magnitude smaller than the first. This somewhat simplifies the final form of the production cross sections. It is also useful to note that the quark model used by us has certain universality, since the quark interaction operator contains the perturbative part based on calculations in the framework of the nonrelativistic QCD and the widely used nonperturbative part [2–4,36,37,39,40].

Performing analytical integration of the differential effective cross sections (22) over the angle θ, we obtain the total cross sections for the production of a pair of mesons. The corresponding expressions are very bulky, so we present here only nonrelativistic cross sections in the form:

$$\sigma_{\mathcal{PP}} = \frac{512\pi^3\alpha^2_{s,c}Q_c^4\alpha^2|\mathbf{P}|}{27r_1^6r_2^6\tilde{s}^7M^9}|\Psi^0_{\mathcal{P}}(0)|^4\left[\sqrt{\tilde{s}}h_1(\tilde{s})+\frac{1}{\sqrt{\tilde{s}-4}}\ln\frac{\sqrt{\tilde{s}}-\sqrt{\tilde{s}-4}}{\sqrt{\tilde{s}}+\sqrt{\tilde{s}-4}}h_2(\tilde{s})\right], \tag{33}$$

$$\begin{aligned}h_1(\tilde{s}) &= 192((q_{bc}-1)^2(q_{bc}^2-34q_{bc}+113)r_1^6+(36q_{bc}^2-220q_{bc}+225)r_1^4-2(q_{bc}^2-40q_{bc}+80)r_1^3\\&+2(4q_{bc}^3-63q_{bc}^2+160q_{bc}-101)r_1^5+5(q_{bc}-1)^4r_1^8-4(q_{bc}-9)(q_{bc}-1)^3r_1^7+(71-12q_{bc})r_1^2-18r_1+2)\\&-(r_1-1)^2r_1^2\tilde{s}^3(q_{bc}^4(72r_1^4-80r_1^3-20r_1^2+44r_1-11)-4q_{bc}^3(72r_1^4-112r_1^3+36r_1^2+24r_1-11)\\&+q_{bc}^2(432r_1^4-864r_1^3+520r_1^2-88r_1-26)-4q_{bc}(72r_1^4-176r_1^3+132r_1^2-48r_1+9)+72r_1^4-208r_1^3\\&+172r_1^2-52r_1+5)+16(r_1-1)r_1\tilde{s}(q_{bc}^4r_1^3(34r_1^3-46r_1^2+15r_1-3)-2q_{bc}^3r_1^2(68r_1^4-148r_1^3+98r_1^2\\&-27r_1+6)+3q_{bc}^2(68r_1^6-204r_1^5+214r_1^4-88r_1^3+17r_1^2-7r_1+1)-2q_{bc}(r_1-1)^2(68r_1^4-124r_1^3+62r_1^2\\&+3r_1-3)+(r_1-1)^3r_1(34r_1^2-56r_1+25))-2\tilde{s}^2(q_{bc}^4r_1^2(72r_1^6-64r_1^5-144r_1^4+228r_1^3-113r_1^2+18r_1-3)\\&-4q_{bc}^3r_1^2(72r_1^6-176r_1^5+160r_1^4-46r_1^3-23r_1^2+16r_1-3)+2q_{bc}^2r_1(216r_1^7-864r_1^6+1568r_1^5-1680r_1^4\\&+1175r_1^3-558r_1^2+173r_1-30)-4q_{bc}(r_1-1)^2r_1(72r_1^5-256r_1^4+360r_1^3-274r_1^2+119r_1-24)+(r_1-1)^2\\&\times(72r_1^6-368r_1^5+616r_1^4-452r_1^3+147r_1^2-12r_1-6))+(q_{bc}-1)^4(r_1-1)^2r_1^2(8r_1^4-16r_1^3+12r_1^2-4r_1+1)\tilde{s}^4,\end{aligned} \tag{34}$$

$$\begin{aligned}h_2(\tilde{s}) &= 6((q_{bc}-1)^2(r_1-1)^2r_1^2\tilde{s}^4(q_{bc}^2(8r_1^4-8r_1^3+4r_1-1)-2q_{bc}(8r_1^4-16r_1^3+8r_1^2-1)+8r_1^4-24r_1^3\\&+24r_1^2-12r_1+3)-2(q_{bc}-1)^2(r_1-1)r_1\tilde{s}^3(-16(2q_{bc}^2-3q_{bc}+1)r_1^5+8(4q_{bc}^2-6q_{bc}-1)r_1^4\\&-16(q_{bc}^2-q_{bc}-3)r_1^3+(5q_{bc}^2-2q_{bc}-51)r_1^2+(-q_{bc}^2+2q_{bc}+23)r_1+8(q_{bc}-1)^2r_1^6-4)+64((q_{bc}-1)^2\\&\times(q_{bc}^2-34q_{bc}+113)r_1^6+(36q_{bc}^2-220q_{bc}+225)r_1^4-2(q_{bc}^2-40q_{bc}+80)r_1^3+2(4q_{bc}^3-63q_{bc}^2+160q_{bc}\end{aligned}$$

$$-101)r_1^5+5(q_{bc}-1)^4r_1^8-4(q_{bc}-9)(q_{bc}-1)^3r_1^7+(71-12q_{bc})r_1^2-18r_1+2)-2\tilde{s}^2(4(q_{bc}-1)^2(5q_{bc}^2-106q_{bc}+173)r_1^6+4(3q_{bc}^4+56q_{bc}^3-330q_{bc}^2+528q_{bc}-257)r_1^5+(-15q_{bc}^4-36q_{bc}^3+606q_{bc}^2-1396q_{bc}+905)r_1^4+2(3q_{bc}^4-8q_{bc}^3-66q_{bc}^2+240q_{bc}-233)r_1^3+(-q_{bc}^4+4q_{bc}^3+6q_{bc}^2-52q_{bc}+123)r_1^2+40(q_{bc}-1)^4r_1^8-64(q_{bc}-4)(q_{bc}-1)^3r_1^7-8(q_{bc}+1)r_1-2)+16\tilde{s}((q_{bc}-1)^2(15q_{bc}^2-110q_{bc}+71)r_1^6+(8q_{bc}^2+16q_{bc}-109)r_1^2-(q_{bc}^2+2q_{bc}-40)r_1+4(q_{bc}^3-8q_{bc}^2-6q_{bc}+37)r_1^3+(-6q_{bc}^4+78q_{bc}^3-246q_{bc}^2+202q_{bc}-28)r_1^5+(q_{bc}^4-22q_{bc}^3+109q_{bc}^2-52q_{bc}-84)r_1^4+8(q_{bc}-1)^4r_1^8-8(q_{bc}-1)^3(3q_{bc}-5)r_1^7-6)), \quad (35)$$

$$\sigma_{\mathcal{VV}}=\frac{1024\pi^3\alpha_{s,c}^2Q_c^4\alpha^2|\mathbf{P}|}{27r_1^6r_2^6\tilde{s}^7M^9}|\Psi_{\mathcal{V}}^0(0)|^4\left[\sqrt{\tilde{s}}h_5(\tilde{s})+\frac{1}{\sqrt{\tilde{s}-4}}\ln\frac{\sqrt{\tilde{s}}-\sqrt{\tilde{s}-4}}{\sqrt{\tilde{s}}+\sqrt{\tilde{s}-4}}h_6(\tilde{s})\right], \quad (36)$$

$$h_5(\tilde{s})=2(q_{bc}^4+6q_{bc}^2+1)(r_1-1)^2r_1^2\tilde{s}^4+48((q_{bc}-1)^2(17q_{bc}^2-302q_{bc}+829)r_1^6+5(54q_{bc}^2-304q_{bc}+303)r_1^4-10(q_{bc}^2-52q_{bc}+104)r_1^3+2(44q_{bc}^3-495q_{bc}^2+1160q_{bc}-709)r_1^5+40(q_{bc}-1)^4r_1^8-4(q_{bc}-1)^3\times(11q_{bc}-69)r_1^7+(451-72q_{bc})r_1^2-114r_1+13)+4(r_1-1)r_1\tilde{s}^3(q_{bc}^4r_1(r_1^3-4r_1^2+10r_1-7)+q_{bc}^3r_1(-4r_1^3+12r_1^2-17r_1+15)+2q_{bc}^2r_1(3r_1^3-6r_1^2+14r_1-11)-q_{bc}(4r_1^4-4r_1^3+5r_1^2+r_1-6)+r_1(r_1^3+4r_1-5))+\tilde{s}^2(8(q_{bc}-1)^2(9q_{bc}^2-67q_{bc}+121)r_1^6+12(8q_{bc}^2-7q_{bc}-3)r_1-4(16q_{bc}^4+9q_{bc}^3+240q_{bc}^2-581q_{bc}+316)r_1^5+(83q_{bc}^4+476q_{bc}^3-358q_{bc}^2-944q_{bc}+843)r_1^4-4(6q_{bc}^4+86q_{bc}^3-131q_{bc}^2+36q_{bc}+53)r_1^3+(24q_{bc}^4+72q_{bc}^3-262q_{bc}^2+296q_{bc}-6)r_1^2+64(q_{bc}-1)^4r_1^8-128(q_{bc}-3)(q_{bc}-1)^3r_1^7+27)+4\tilde{s}(-4(q_{bc}-1)^2(25q_{bc}^2-445q_{bc}+963)r_1^6+2(69q_{bc}^2+162q_{bc}-599)r_1^2-6(4q_{bc}^2+q_{bc}-37)r_1+4(24q_{bc}^3-51q_{bc}^2-553q_{bc}+852)r_1^3-2(9q_{bc}^4+209q_{bc}^3-2532q_{bc}^2+5339q_{bc}-3025)r_1^5+(15q_{bc}^4-234q_{bc}^3-1206q_{bc}^2+6656q_{bc}-5775)r_1^4-208(q_{bc}-1)^4r_1^8+8(q_{bc}-1)^3(37q_{bc}-171)r_1^7-15), \quad (37)$$

$$h_6(\tilde{s})=6(16((q_{bc}-1)^2(17q_{bc}^2-302q_{bc}+829)r_1^6+5(54q_{bc}^2-304q_{bc}+303)r_1^4-10(q_{bc}^2-52q_{bc}+104)r_1^3+2(44q_{bc}^3-495q_{bc}^2+1160q_{bc}-709)r_1^5+40(q_{bc}-1)^4r_1^8-4(q_{bc}-1)^3(11q_{bc}-69)r_1^7+(451-72q_{bc})r_1^2-114r_1+13)+\tilde{s}^2(8(q_{bc}-1)^2(7q_{bc}^2-64q_{bc}+147)r_1^6-8(2q_{bc}^2-8q_{bc}+17)r_1+4(7q_{bc}^4+6q_{bc}^3-348q_{bc}^2+818q_{bc}-483)r_1^5+(-43q_{bc}^4+248q_{bc}^3+294q_{bc}^2-2272q_{bc}+2057)r_1^4-4(2q_{bc}^4+30q_{bc}^3+15q_{bc}^2-266q_{bc}+361)r_1^3+(8q_{bc}^4+24q_{bc}^3+70q_{bc}^2-352q_{bc}+622)r_1^2+64(q_{bc}-1)^4r_1^8-32(q_{bc}-1)^3(3q_{bc}-13)r_1^7+9)-4\tilde{s}(2(q_{bc}-1)^2(35q_{bc}^2-372q_{bc}+931)r_1^6-2(23q_{bc}^2+78q_{bc}-540)r_1^2+2(4q_{bc}^2+q_{bc}-151)r_1-4(8q_{bc}^3-28q_{bc}^2-271q_{bc}+584)r_1^3+6(q_{bc}^4+33q_{bc}^3-366q_{bc}^2+851q_{bc}-519)r_1^5+(-5q_{bc}^4+78q_{bc}^3+430q_{bc}^2-3232q_{bc}+3315)r_1^4+96(q_{bc}-1)^4r_1^8-128(q_{bc}-5)(q_{bc}-1)^3r_1^7+39)+8(q_{bc}-1)^2q_{bc}(r_1-1)^2r_1^2\tilde{s}^3), \quad (38)$$

where $\sqrt{\tilde{s}}=\sqrt{s}/M=\sqrt{s}/(m_1+m_2)$, $q_{bc}=Q_b\alpha_{s,c}/Q_c\alpha_{s,b}$. From these expressions, the general structure of the production cross sections is clearly visible: they are determined by functions that are an expansion in two parameters r_1 and q_{bc} at a given energy s. The terms with relativistic corrections have the same form.

The type of total production cross sections $\sigma_{\mathcal{PP}}$ and $\sigma_{\mathcal{VV}}$ depending on center-of-mass energy $\sqrt{s}$ is shown in Fig. 3, on which we demonstrate a comparison of results of nonrelativistic and relativistic calculation. In general, the type of cross sections for pair production of mesons remains the same as for other reactions e^+e^- annihilation and pp-interaction. At the threshold, the cross sections vanish due to the $|\mathbf{P}|$ factor. In our calculations, we did not take into account the Coulomb interaction of particles in the final state. The ILC project plans to achieve high energies of order $\sqrt{s}=100$ GeV or more. In this paper, we present the numerical values of the production cross sections at relatively low energies (see Fig. 3), bearing in mind that measurements at such energies will also be possible. But our general formulas (33), (36) allow us to make a numerical calculation at any energies.

The production of a pair of B_c mesons in e^+e^- annihilation was considered by us earlier in [20,21].

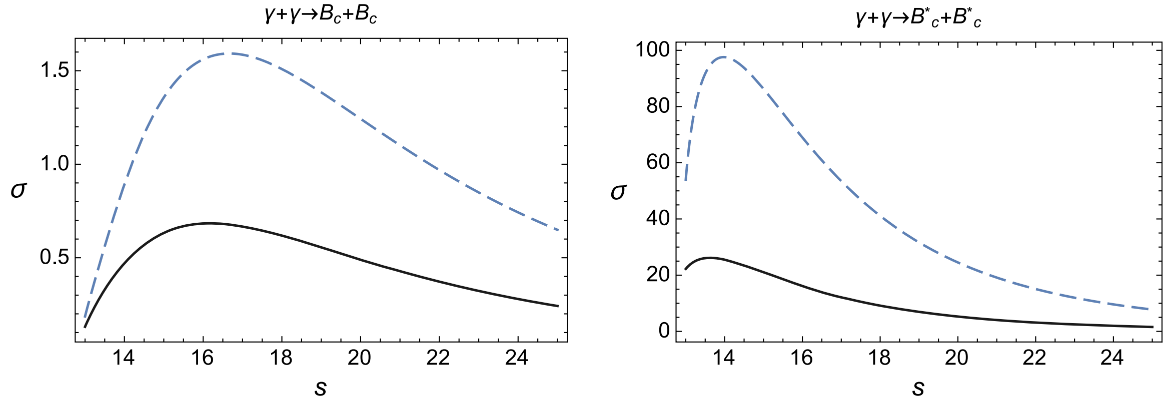

FIG. 3. The cross section σ in fb of pair B_c meson production in $\gamma\gamma$ interaction as a function of the center-of-mass energy $\sqrt{s}$ in GeV (solid line). The dashed line shows nonrelativistic result.

In these works, both single-photon and two-photon meson pair production mechanisms were investigated. The cross section for the production of a pair of B_c mesons in e^+e^- annihilation in processes with two virtual photons is suppressed with respect to the cross section obtained in the single-photon mechanism by an additional α^2 factor. In the reaction $\gamma\gamma \to B_c^+ B_c^-$ with two real photons, the general factor in the cross sections (32), (35) is the same as in electron-positron annihilation with one virtual photon. Nevertheless, the numerical results presented in Fig. 3 show that the cross section $\sigma_{\mathcal{VV}}(\gamma\gamma \to B_c^+ B_c^-)$ is more than an order of magnitude larger the cross section $\sigma_{\mathcal{VV}}(e^+e^- \to \gamma^* \to B_c^+ B_c^-)$ (single-photon annihilation mechanism [20]). The cross section $\sigma_{\mathcal{PP}}(\gamma\gamma \to B_c^+ B_c^-)$ is 10 times larger than the cross section $\sigma_{\mathcal{PP}}(e^+e^- \to \gamma^* \to B_c^+ B_c^-)$ [20]. First of all, it should be noted that a significant increase in the cross section for the production of a pair of vector mesons as compared to other mesons is also observed in e^+e^- annihilation [19,20,41]. The increase in the cross section for the production of a pair of vector mesons during the transition from the reaction $e^+e^- \to B_c^{*+} B_c^{*-}$ to the process $\gamma\gamma \to B_c^{*+} B_c^{*-}$ is due to the structure of total amplitude, which is determined by 20 Feynman diagrams. Thus, we can say that the observation of the pair production of vector B_c^* mesons in the $\gamma\gamma$ interaction has clear advantages. Our results are in agreement with previous calculation made in [19] in a nonrelativistic approach. So, for example, the numerical value of the production cross section $\sigma_{\mathcal{VV}}$ from [19] at the maximum point is near $10^{-7}\mu b$ what is close to our nonrelativistic values in Fig. 3 (dashed line). A slight difference in nonrelativistic results is related to the choice of parameters $\Psi_{B_c}(0)$ and α_s. Assuming that the luminosity of the photon collider will be at least half the luminosity of the electron-positron collider ($\sim 10^{34}$ cm^{-2} c^{-1}), we can estimate the yield of pairs of vector B_c mesons at 250 events per month. It is obtained by multiplying the calculated pair production cross section at $\sqrt{s} = 15$ GeV and the estimated luminosity of the photon collider.

In conclusion, we list the main theoretical uncertainties of our calculation. The calculation of all the main parameters that determine the cross sections for the production of a pair of B_c mesons is performed within the framework of the quark model (see also [20,21]). Moreover, we did not take into account the contribution from the parameters ω_{20}, ω_{02}, ω_{11}, which in principle can be taken into account. They are related to corrections of order $\mathbf{p}^4/m_{1,2}^4$, $\mathbf{q}^4/m_{1,2}^4$. Their contribution to the production cross section can be about 30%. Another important source of theoretical error is related to the determination of the wave function of the bound states of quarks in the region of relativistic momenta. Taking into account the contribution of the relativistic momentum region to the total value of parameters (28), we can say that the possible theoretical error in the cross section does not exceed 20% (the error in the wave function is estimated at 5%). Also, in our work, the radiation corrections of order $O(\alpha_s)$, which can be of order 20% in the pair production cross section, were not taken into account. As a result, we estimate the total theoretical uncertainty of our calculations at approximately 40%. When our work was already published in the electronic archive, a work [42] appeared in which one-loop corrections to the pair production cross section were calculated. Direct comparison of our results with the work [42] is difficult, since we study the dependence of the cross sections on the total energy $\sqrt{s}$, which in our work has much smaller values. The results of [42], obtained at energies of $\sqrt{s} = 250$ GeV and $\sqrt{s} = 500$ GeV, show that taking NLO corrections into account leads to a significant decrease in the production cross sections as compared to the result in the leading order (see Fig. 3 [42]). Thus, the results of our work and [42] confirm the conclusion known in the study of the quarkonia production in electron-positron annihilation that the relativistic corrections and the radiative corrections of order $O(\alpha_s)$ are the two most important factors that must be taken into account when obtaining the production cross sections for the pair of B_c mesons.

ACKNOWLEDGMENTS

The authors are grateful to A. V. Berezhnoy for useful discussions. The work of F. A. M. is supported by the Foundation for the Advancement of Theoretical Physics and Mathematics "BASIS" (Grant No. 19-1-5-67-1).

APPENDIX A: THE FEYNMAN AMPLITUDES OF A PRODUCTION OF HEAVY b, c QUARKS AND $\bar{b}$,$\bar{c}$ ANTIQUARKS IN $\gamma\gamma$ INTERACTION

At the first perturbative stage of the process of production of a B_c meson pair that we are studying, we have the production of two heavy quarks (b, c) and two heavy antiquarks $(\bar{b}, \bar{c})$ in the photon-photon interaction. In the leading order in α_s, this stage is described by 20 Feynman amplitudes in Fig. 4, which can be generated in the FeynArts package [26]. At the second stage of the production process, quarks and antiquarks unite with some probability into B_c mesons. The part of the Feynman amplitudes in this stage is presented in Fig. 1.

APPENDIX B: THE COEFFICIENT FUNCTIONS $A_i^{\mu\nu}$ ENTERING IN THE PSEUDOSCALAR B_c MESON PRODUCTION AMPLITUDE (19)

$\gamma + \gamma \to B_c^+ + B_c^-$.

$$A_i^{\mu\nu} = f_{i,1} v_1^\mu v_1^\nu + f_{i,2} g^{\mu\nu}, \tag{B1}$$

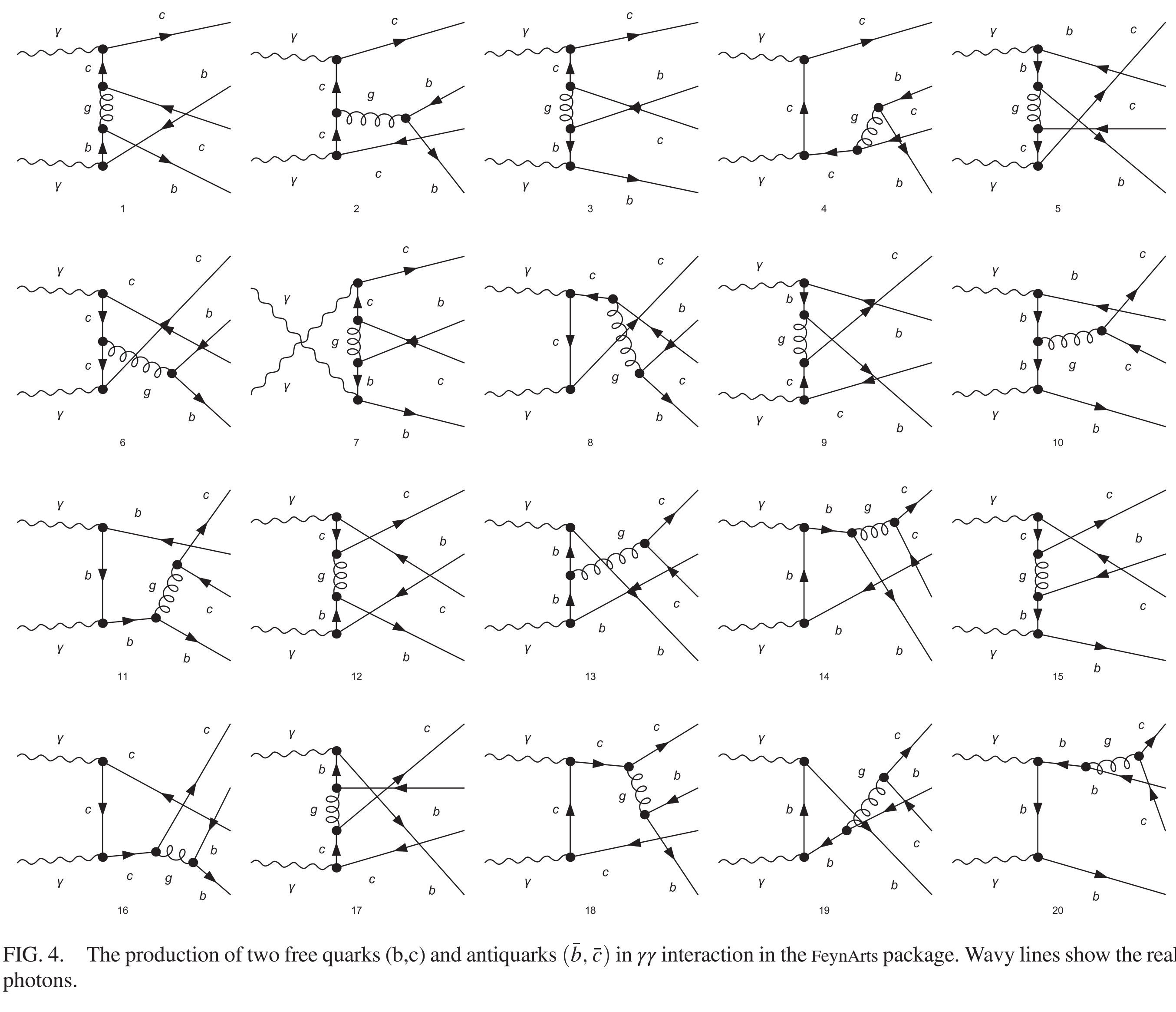

FIG. 4. The production of two free quarks (b,c) and antiquarks $(\bar{b}, \bar{c})$ in $\gamma\gamma$ interaction in the FeynArts package. Wavy lines show the real photons.

$$
\begin{aligned}
f_{1,1} = {} & c_1\left(s\left(q_b^2\left(-\frac{64r_1^4}{3}-\frac{128r_1^3}{3}\right)+q_c^2\left(-\frac{128r_1^4}{3}+\frac{128r_1^3}{3}+\frac{128r_1^2}{3}-\frac{128r_1}{3}\right)\right)-\frac{64}{3}q_b^2r_1^4\right.\\
& \left.+q_c^2(512r_1^4-1664r_1^3+1920r_1^2-896r_1+128)\right)+c_2\left(s\left(q_b^2\left(-\frac{128r_1^4}{3}+128r_1^3-\frac{256r_1^2}{3}\right)\right.\right.\\
& \left.\left.+q_c^2\left(-\frac{64r_1^4}{3}+128r_1^3-256r_1^2+\frac{640r_1}{3}-64\right)\right)+q_b^2(512r_1^4-384r_1^3)+q_c^2\left(-\frac{64r_1^4}{3}+\frac{256r_1^3}{3}-128r_1^2\right.\right.\\
& \left.\left.+\frac{256r_1}{3}-\frac{64}{3}\right)\right)+s(q_b^2(32r_1^3-32r_1^4)+q_c^2(-32r_1^4+96r_1^3-96r_1^2+32r_1))-64q_b^2r_1^4+q_c^2(-64r_1^4\\
& +256r_1^3-384r_1^2+256r_1-64),
\end{aligned}
\tag{B2}
$$

$$
\begin{aligned}
f_{1,2} = {} & \sqrt{c_1}\sqrt{c_2}(|\mathbf{P}|s^{3/2}z(16q_b^2r_1^2+q_c^2(16r_1^2-32r_1+16))+s^2(q_c^2(-8r_1^2+16r_1-8)-8q_b^2r_1^2)\\
& +s(48q_b^2r_1^2+48q_c^2(1-r_1)^2))+c_1\left(|\mathbf{P}|z\left(s^{3/2}\left(q_b^2\left(16r_1^2-\frac{32r_1^3}{3}\right)+q_c^2\left(-\frac{16r_1^3}{3}+\frac{32r_1^2}{3}-\frac{16r_1}{3}\right)\right)\right.\right.\\
& \left.+\sqrt{s}(q_c^2(128r_1^3-288r_1^2+192r_1-32)-16q_b^2r_1^3)\right)+s^2\left(q_b^2\left(\frac{16r_1^3}{3}-8r_1^2\right)+q_c^2\left(\frac{8r_1^3}{3}-\frac{16r_1^2}{3}+\frac{8r_1}{3}\right)\right)\\
& \left.+s\left(q_b^2\left(\frac{32r_1^4}{3}+\frac{56r_1^3}{3}-16r_1^2\right)-\frac{256}{3}r_1q_c^2(r_1-1)^2\right)+\frac{64q_b^2r_1^4}{3}\right)+c_2\left(|\mathbf{P}|z\left(s^{3/2}\left(\frac{16}{3}q_b^2r_1^2(r_1-1)\right.\right.\right.\\
& \left.\left.\left.+q_c^2\left(\frac{32r_1^3}{3}-16r_1^2+\frac{16}{3}\right)\right)+\sqrt{s}(q_b^2(96r_1^2-128r_1^3)+16q_c^2(r_1^3-3r_1^2+3r_1-1))\right)\right)+s^2\left(\frac{8}{3}q_b^2r_1^2(1-r_1)\right.\\
& \left.+q_c^2\left(-\frac{16r_1^3}{3}+8r_1^2-\frac{8}{3}\right)\right)+s\left(q_b^2\left(\frac{256r_1^3}{3}-\frac{256r_1^2}{3}\right)+q_c^2\left(\frac{32r_1^4}{3}-\frac{184r_1^3}{3}+104r_1^2-\frac{200r_1}{3}+\frac{40}{3}\right)\right)\\
& \left.+q_c^2\left(\frac{64r_1^4}{3}-\frac{256r_1^3}{3}+128r_1^2-\frac{256r_1}{3}+\frac{64}{3}\right)\right)+|\mathbf{P}|z(s^{3/2}(q_b^2(8r_1^3-8r_1^2)+q_c^2(-8r_1^3+16r_1^2-8r_1))\\
& +\sqrt{s}(16q_b^2r_1^3+q_c^2(-16r_1^3+48r_1^2-48r_1+16)))+s^4(q_b^2(4r_1^2-4r_1^3)+q_c^2(4r_1^3-8r_1^2+4r_1))\\
& +s(q_b^2(8r_1^2-8r_1^3)+q_c^2(8r_1^3-16r_1^2+8r_1)),
\end{aligned}
\tag{B3}
$$

$$
\begin{aligned}
f_{2,1} = {} & \sqrt{c_1}\sqrt{c_2}s(-16q_b^2-16q_c^2)+c_1\left(s\left(q_b^2\left(-\frac{64r_1^2}{3}+\frac{64r_1}{3}-16\right)+q_bq_c\left(\frac{32r_1^2}{3}+\frac{32r_1}{3}-32\right)\right.\right.\\
& \left.\left.+q_c^2\left(32r_1^2+\frac{64r_1}{3}-16\right)\right)-32q_b^2r_1^2+q_bq_c(64r_1-256r_1^2)+q_c^2(-224r_1^2+320r_1-64)\right)\\
& +c_2\left(s\left(q_b^2\left(32r_1^2-\frac{256r_1}{3}+\frac{112}{3}\right)+q_bq_c\left(\frac{32r_1^2}{3}-32r_1-\frac{32}{3}\right)+q_c^2\left(-\frac{64r_1^2}{3}+\frac{64r_1}{3}-16\right)\right)\right.\\
& \left.+q_b^2(-224r_1^2+128r_1+32)+q_bq_c(-256r_1^2+448r_1-192)+q_c^2(-32r_1^2+64r_1-32)\right)\\
& +s(q_b^2(16r_1^2-16r_1+8)+q_bq_c(32r_1^2-32r_1+16)+q_c^2(16r_1^2-16r_1+8))\\
& +32q_b^2r_1^2+q_bq_c(64r_1^2-64r_1)+q_c^2(32r_1^2-64r_1+32),
\end{aligned}
\tag{B4}
$$

$$f_{2,2} = \sqrt{c_1}\sqrt{c_2}(|\mathbf{P}|^2 s z^2(8q_b^2+8q_c^2)+16|\mathbf{P}|q_b q_c s^{3/2}z+s^2(-2q_b^2-8q_bq_c-2q_c^2) + s(8q_b^2+16q_bq_c+8q_c^2)) + c_1\left(|\mathbf{P}|^2 s z^2(8q_b^2+8q_c^2)+|\mathbf{P}|z\left(\sqrt{s}\left(\frac{16q_b^2r_1}{3}-16q_bq_cr_1+\frac{32q_c^2r_1}{3}\right) + 16q_bq_cs^3\right)+s\left(q_b^2\left(8-\frac{8r_1}{3}\right)+8q_bq_c(r_1+2)+q_c^2\left(8-\frac{16r_1}{3}\right)\right)-2s^2(q_b^2+4q_bq_c+q_c^2)\right) + c_2\left(|\mathbf{P}|^2 s z^2(8q_b^2+8q_c^2)+|\mathbf{P}|z\left(\sqrt{s}\left(\frac{32}{3}q_b^2(1-r_1)+16q_bq_c(r_1-1)+\frac{16}{3}q_c^2(1-r_1)\right)+16q_bq_cs^3\right) + s\left(\frac{8}{3}q_b^2(2r_1+1)+8q_bq_c(3-r_1)+\frac{8}{3}q_c^2(r_1+2)\right)-2s^2(q_b^2+4q_bq_c+q_c^2)\right)-4|\mathbf{P}|^2sz^2(q_b^2+q_c^2) - 8|\mathbf{P}|q_bq_cs^{3/2}z+s^2(q_b^2+4q_bq_c+q_c^2)+s(-4q_b^2-8q_bq_c-4q_c^2), \tag{B5}$$

$$f_{3,1} = c_1\left(s\left(q_b^2\left(-\frac{64r_1^4}{3}-\frac{128r_1^3}{3}\right)+q_c^2\left(-\frac{128r_1^4}{3}+\frac{128r_1^3}{3}+\frac{128r_1^2}{3}-\frac{128r_1}{3}\right)\right)-\frac{64}{3}q_b^2r_1^4+q_c^2(512r_1^4-1664r_1^3 + 1920r_1^2-896r_1+128)\right)+c_2\left(s\left(q_b^2\left(-\frac{128r_1^4}{3}+128r_1^3-\frac{256r_1^2}{3}\right)+q_c^2\left(-\frac{64r_1^4}{3}+128r_1^3-256r_1^2+\frac{640r_1}{3}-64\right)\right) + q_b^2(512r_1^4-384r_1^3)+q_c^2\left(-\frac{64r_1^4}{3}+\frac{256r_1^3}{3}-128r_1^2+\frac{256r_1}{3}-\frac{64}{3}\right)\right)+s(q_b^2(32r_1^3-32r_1^4) + q_c^2(-32r_1^4+96r_1^3-96r_1^2+32r_1))-64q_b^2r_1^4+q_c^2(-64r_1^4+256r_1^3-384r_1^2+256r_1-64), \tag{B6}$$

$$f_{3,2} = \sqrt{c_1}\sqrt{c_2}(|\mathbf{P}|s^{3/2}z(q_c^2(-16r_1^2+32r_1-16)-16q_b^2r_1^2)+s^2(q_c^2(-8r_1^2+16r_1-8)-8q_b^2r_1^2) + s(48q_b^2r_1^2+q_c^2(48r_1^2-96r_1+48)))+c_1\left(|\mathbf{P}|z\left(s^{3/2}\left(q_b^2\left(\frac{32r_1^3}{3}-16r_1^2\right)+q_c^2\left(\frac{16r_1^3}{3}-\frac{32r_1^2}{3}+\frac{16r_1}{3}\right)\right) + \sqrt{s}(16q_b^2r_1^3+q_c^2(-128r_1^3+288r_1^2-192r_1+32))\right)+s^2\left(q_b^2\left(\frac{16r_1^3}{3}-8r_1^2\right)+q_c^2\left(\frac{8r_1^3}{3}-\frac{16r_1^2}{3}+\frac{8r_1}{3}\right)\right) + s\left(q_b^2\left(\frac{32r_1^4}{3}+\frac{56r_1^3}{3}-16r_1^2\right)+q_c^2\left(-\frac{256r_1^3}{3}+\frac{512r_1^2}{3}-\frac{256r_1}{3}\right)\right)+\frac{64q_b^2r_1^4}{3}\right)+c_2\left(|\mathbf{P}|z\left(s^{3/2}\left(q_b^2\left(\frac{16r_1^2}{3} - \frac{16r_1^3}{3}\right)+q_c^2\left(-\frac{32r_1^3}{3}+16r_1^2-\frac{16}{3}\right)\right)+\sqrt{s}\left(q_b^2(128r_1^3-96r_1^2)+16q_c^2(1-r_1)^3+s^2\left(q_b^2\left(\frac{8r_1^2}{3}-\frac{8r_1^3}{3}\right) + q_c^2\left(-\frac{16r_1^3}{3}+8r_1^2-\frac{8}{3}\right)\right)+s\left(q_b^2\left(\frac{256r_1^3}{3}-\frac{256r_1^2}{3}\right)+q_c^2\left(\frac{32r_1^4}{3}-\frac{184r_1^3}{3}+104r_1^2-\frac{200r_1}{3}+\frac{40}{3}\right)\right) + q_c^2\left(\frac{64r_1^4}{3}-\frac{256r_1^3}{3}+128r_1^2-\frac{256r_1}{3}+\frac{64}{3}\right)\right)+|\mathbf{P}|z(s^{3/2}(8q_b^2r_1^2(1-r_1)+8q_c^2r_1(r_1-1)^2+\sqrt{s}(q_c^2(16r_1^3-48r_1^2 + 48r_1-16)-16q_b^2r_1^3))+s^2(4q_b^2r_1^2(1-r_1)+4r_1q_c^2(1-r_1)^2)+s(q_b^2(8r_1^2-8r_1^3)+q_c^2(8r_1^3-16r_1^2+8r_1)), \tag{B7}$$

$$f_{4,1} = -16\sqrt{c_1}\sqrt{c_2}s(q_b^2+q_c^2)+c_1\left(s\left(q_b^2\left(-\frac{64r_1^2}{3}+\frac{64r_1}{3}-16\right)+q_bq_c\left(\frac{32r_1^2}{3}+\frac{32r_1}{3}-32\right) + q_c^2\left(32r_1^2+\frac{64r_1}{3}-16\right)\right)-32q_b^2r_1^2+q_bq_c(64r_1-256r_1^2)+q_c^2(-224r_1^2+320r_1-64)\right) + c_2\left(s\left(q_b^2\left(32r_1^2-\frac{256r_1}{3}+\frac{112}{3}\right)+q_bq_c\left(\frac{32r_1^2}{3}-32r_1-\frac{32}{3}\right)+q_c^2\left(-\frac{64r_1^2}{3}+\frac{64r_1}{3}-16\right)\right) + q_b^2(-224r_1^2+128r_1+32)+q_bq_c(-256r_1^2+448r_1-192)+q_c^2(-32r_1^2+64r_1-32)\right) + s(q_b^2(16r_1^2-16r_1+8)+q_bq_c(32r_1^2-32r_1+16)+q_c^2(16r_1^2-16r_1+8))+32q_b^2r_1^2 + q_bq_c(64r_1^2-64r_1)+q_c^2(32r_1^2-64r_1+32), \tag{B8}$$

$$f_{4,2} = \sqrt{c_1}\sqrt{c_2}(|\mathbf{P}|^2 s z^2(8q_b^2+8q_c^2) - 16|\mathbf{P}|q_b q_c s^{3/2} z + s^2(-2q_b^2 - 8q_b q_c - 2q_c^2) + s(8q_b^2+16q_b q_c+8q_c^2)) + c_1\left(|\mathbf{P}|^2 s z^2(8q_b^2+8q_c^2) + |\mathbf{P}|z\left(\sqrt{s}\left(-\frac{16q_b^2 r_1}{3} + 16 q_b q_c r_1 - \frac{32 q_c^2 r_1}{3}\right) - 16 q_b q_c s^{3/2}\right) + s\left(q_b^2\left(8-\frac{8r_1}{3}\right) + q_b q_c(8r_1+16) + q_c^2\left(8 - \frac{16r_1}{3}\right)\right) + s^2(-2q_b^2 - 8q_b q_c - 2q_c^2)\right) + c_2\left(8|\mathbf{P}|^2 s z^2(q_b^2+q_c^2) + |\mathbf{P}|z\left(\sqrt{s}\left(\frac{32}{3}q_b^2(r_1-1) + 16q_b q_c(1-r_1) + \frac{16}{3}q_c^2(r_1-1)\right) - 16q_b q_c s^{3/2}\right) + s\left(q_b^2\left(\frac{16r_1}{3}+\frac{8}{3}\right) + q_b q_c(24-8r_1) + q_c^2\left(\frac{8r_1}{3}+\frac{16}{3}\right)\right) + s^2(-2q_b^2 - 8q_b q_c - 2q_c^2)\right) + |\mathbf{P}|^2 s z^2(-4q_b^2 - 4q_c^2) + 8|\mathbf{P}|q_b q_c s^{3/2} z + s^2(q_b^2 + 4q_b q_c + q_c^2) + s(-4q_b^2 - 8q_b q_c - 4q_c^2), \tag{B9}$$

$$f_{5,1} = -64\sqrt{c_1}\sqrt{c_2}q_b q_c s + c_1\left(q_b q_c\left(-64r_1^2 - \frac{64r_1}{3}\right)s + q_b q_c\left(\frac{1280 r_1^2}{3} - 128 r_1\right)\right) + c_2\left(q_b q_c\left(-64r_1^2 + \frac{448 r_1}{3} - \frac{256}{3}\right)s^2 + q_b q_c\left(\frac{1280r_1^2}{3} - \frac{2176 r_1}{3} + \frac{896}{3}\right)\right) + q_b q_c(64r_1 - 64r_1^2)s + q_b q_c(128 r_1 - 128 r_1^2), \tag{B10}$$

$$f_{5,2} = \sqrt{c_1}\sqrt{c_2}(32|\mathbf{P}|^2 q_b q_c s z^2 - 8q_b q_c s^2 + 96 q_b q_c s) + c_1\left(32|\mathbf{P}|^2 q_b q_c s z^2 + q_b q_c\left(\frac{128r_1^2}{3} - \frac{80r_1}{3} - 32\right)s + \frac{256}{3}q_b q_c r_1^2 - 8q_b q_c s^2\right) + c_2\left(32|\mathbf{P}|^2 q_b q_c s z^2 + q_b q_c\left(\frac{128r_1^2}{3} - \frac{176r_1}{3} - 16\right)s^2 + q_b q_c\left(\frac{256r_1^2}{3} - \frac{512r_1}{3} + \frac{256}{3}\right) - 8q_b q_c s^4\right) - 16|\mathbf{P}|^2 q_b q_c s z^2 + 4q_b q_c s^2 + 16 q_b q_c s, \tag{B11}$$

In all these equations the substitution $q_c \to Q_c\sqrt{\alpha_{s,b}}$, $q_b \to Q_b\sqrt{\alpha_{s,c}}$ is needed. In these expressions, the role of relativistic corrections is played by the functions $c_1(q) = (\varepsilon_1(q) - m_1)/(\varepsilon_1(q) + m_1)$, $c_2(q) = (\varepsilon_2(q) - m_2)/(\varepsilon_2(q) + m_2)$, which are subsequently converted into relativistic parameters (28).

[1] S. S. Gershtein, V. V. Kiselev, A. K. Likhoded, and A. V. Tkabladze, Phys. Usp. **38**, 1 (1995).
[2] N. Brambilla, S. Eidelman, B. K. Heltsley *et al.*, Eur. Phys. J. C **71**, 1534 (2011).
[3] D. Ebert, R. N. Faustov, and V. O. Galkin, Phys. Rev. D **67**, 014027 (2003).
[4] N. Brambilla, A. Pineda, J. Soto, and A. Vairo, Phys. Rev. D **63**, 014023 (2000).
[5] E. J. Eichten and C. Quigg, Phys. Rev. D **99**, 054025 (2019).
[6] E. Braaten and J. Lee, Phys. Rev. D **67**, 054007 (2003); **72**, 099901(E) (2005).
[7] K.-Y. Liu, Z.-G. He, and K.-T. Chao, Phys. Lett. B **557**, 45 (2003).
[8] G. T. Bodwin, D. Kang, and J. Lee, Phys. Rev. D **74**, 014014 (2006).
[9] D. Ebert and A. P. Martynenko, Phys. Rev. D **74**, 054008 (2006).
[10] D. Ebert, R. N. Faustov, V. O. Galkin, and A. P. Martynenko, Phys. Lett. B **672**, 264 (2009).
[11] K. Hagiwara, E. Kou, and C.-F. Qiao, Phys. Lett. B **570**, 39 (2003).
[12] I. F. Ginzburg, G. L. Kotkin, V. G. Serbo, and V. I. Tel'nov, JETP Lett. **34**, 491 (1981), http://www.jetpletters.ac.ru/ps/1533/article_23442.shtml.
[13] E. A. Kuraev, A. Schiller, and V. G. Serbo, Phys. Lett. **134**, 455 (1984).
[14] C. Brikporad, R. H. Milburn, N. Tanaka, and M. Fotino, Phys. Rev. **138**, B1546 (1965).
[15] V. I. Telnov, Nucl. Part. Phys. Proc. **273–275**, 219 (2016).
[16] B. Badelek *et al.*, Int. J. Mod. Phys. A **19**, 5097 (2004).
[17] A. V. Berezhnoy, A. K. Likhoded, and M. V. Shevlyagin, Phys. Lett. B **342**, 351 (1995).
[18] A. V. Berezhnoy, V. V. Kiselev, and A. K. Likhoded, Phys. Lett. B **381**, 341 (1996).

[19] S. P. Baranov, Phys. Rev. D **55**, 2756 (1997).
[20] A. A. Karyasov, A. P. Martynenko, and F. A. Martynenko, Nucl. Phys. **B911**, 36 (2016).
[21] A. V. Berezhnoy, A. P. Martynenko, F. A. Martynenko, and O. S. Sukhorukova, Nucl. Phys. **A986**, 34 (2019).
[22] M. Tanabashi *et al.* (Particle Data Group), Phys. Rev. D **98**, 030001 (2018).
[23] R. Aaij *et al.* (LHCb Collaboration), Phys. Rev. Lett. **122**, 232001 (2019).
[24] A. V. Berezhnoy, I. N. Belov, A. K. Likhoded, and A. V. Luchinsky, Mod. Phys. Lett. A **34**, 1950331 (2019).
[25] R. Aaij *et al.* (LHCb Collaboration), arXiv:2004.08163v1.
[26] J. Kublbeck, M. Böhm, and A. Denner, Comput. Phys. Commun. **60**, 165 (1990).
[27] T. Hahn, Comput. Phys. Commun. **140**, 418 (2001).
[28] E. N. Elekina and A. P. Martynenko, Phys. Rev. D **81**, 054006 (2010).
[29] A. P. Martynenko and A. M. Trunin, Phys. Rev. D **86**, 094003 (2012).
[30] S. J. Brodsky and J. R. Primack, Ann. Phys. (N.Y.) **52**, 315 (1969).
[31] R. N. Faustov, Ann. Phys. (N.Y.) **78**, 176 (1973).
[32] G. T. Bodwin and A. Petrelli, Phys. Rev. D **66**, 094011 (2002).
[33] A. P. Martynenko, Phys. Rev. D **72**, 074022 (2005).
[34] A. P. Martynenko and A. M. Trunin, Eur. Phys. J. C **75**, 138 (2015).
[35] J. Kuipers, T. Ueda, J. A. M. Vermaseren, and J. Vollinga, Comput. Phys. Commun. **184**, 1453 (2013).
[36] S. F. Radford and W. W. Repko, Phys. Rev. D **75**, 074031 (2007).
[37] S. N. Gupta, J. M. Johnson, W. W. Repko, and C. J. Suchyta, Phys. Rev. D **49**, 1551 (1994).
[38] D. Ebert, R. N. Faustov, and V. O. Galkin, Phys. Rev. D **72**, 034026 (2005).
[39] S. Godfrey, Phys. Rev. D **70**, 054017 (2004).
[40] W. Lucha and F. F. Schöberl, Phys. Rev. A **51**, 4419 (1995).
[41] G. T. Bodwin, J. Lee, and E. Braaten, Phys. Rev. D **67**, 054023 (2003); **72**, 099904(E) (2005).
[42] Z.-Q. Chen, H. Yang, and C.-F. Qiao, Phys. Rev. D **102**, 016011 (2020).